Electronic Supporting Information (ESI) for

Design of three-dimensional electrocatalytic all-in-one electrodes by leveraging electrospinning and calcination approaches

Yaovi Holade,*[a] Zahra Hagheh Kavousi,[a,b] Massomeh Ghorbanloo,[b] Nathalie Masquelez,[a] Sophie Tingry[b] and David Cornu*[a]

[a] *Institut Européen des Membranes, IEM, UMR 5635, Univ Montpellier, ENSCM, CNRS, 34090 Montpellier, France.*

[b] *Department of Chemistry, Faculty of Sciences, University of Zanjan, Zanjan, Iran*

Corresponding authors : E-mail: yaovi.holade@enscm.fr (Y.H.), david.cornu@umontpellier.fr (D.C.).

Table of Contents

EXPERIMENTAL METHODS

Materials and Chemicals. Polyacrylonitrile [PAN, average Mw 150,000 (Typical), Sigma-Aldrich], N,N-dimethylformamide (DMF, suitable for HPLC, ≥99.9%, Sigma-Aldrich), nickel (II) nitrate hexahydrate [$Ni(NO_3)_2{\cdot}6H_2O$, 99%, Acros Organics], nickel (II) acetate [$Ni(CH_3COO)_2{\cdot}4H_2O$, 99%, Acros Organics], nickel (II) sulphate ($NiSO_4{\cdot}6H_2O$, 99%, Merck), nickel (II) phosphate [$Ni_3(PO_4)_2{\cdot}xH_2O$, 98%, Alfa Aesar], nickel (II) acetylacetonate [$Ni(acac)_2$ $Ni(C_4H_7COO)_2$, 95%, Alfa Aesar], potassium nitrate (KNO_3, 99.0% min, Sigma-Aldrich), potassium hexacyanoferrate ($K_3[Fe(CN)_6]$, ≥99.0%, Sigma-Aldrich), potassium permanganate ($KMnO_4$, ≥99%, Sigma-Aldrich), hydrogen peroxide solution (H_2O_2, 30%, Sigma-Aldrich), sulfuric acid (H_2SO_4, 97%, Honeywell), nitric acid (HNO_3, 65%, Sigma-Aldrich), and potassium hydroxide [KOH, 99.98% (trace metal basis), Acros Organics], isopropanol (99.5%, Sigma Aldrich), Nafion® suspension (5 wt%, Sigma Aldrich), and commercial catalyst Pt/C (20 wt%, 2 nm, Premetek Co., USA) were used as-received. N_2 (grade 4.5) gas was purchased from Air Liquide (France) and used as-received. Ultrapure water (18.2 MΩ cm at 20 °C) was produced by a Milli-Q Millipore source (MQ).

Solution formulation. To fabricate PAN-Ni mat, DMF (8 mL) was pre-heated at 80 °C and PAN (1 g) was slowly added under stirring for 15 min. Meanwhile, to target 10-12 wt% of nickel content in the final material (i.e. after electrospinning, stabilization and calcination), nickel (II) precursor (273, 234, 247, 348, and 252 mg for nitrate, acetate, sulphate, phosphate and acetylacetonate, respectively) was dissolved in DMF (2 mL) under stirring at room temperature for 10 min. This second solution was added to the first solution. We note that for the control synthesis, i.e., in the absence of nickel species, 10 mL was used for the first solution (no need of a second solution). The viscous mixture was aged for 12 h at 80 °C under stirring. The solution was then removed from the heating batch and left to cool down to room temperature before the next step.

Electrospinning. The above solution was loaded into a 15 mL syringe. The used infusion pump (KD Scientific) was set to stop at after 8 mL. The grounded counter electrode was connected to an aluminium foil that covers the drum of a diameter of 10 cm and rotating at 1000 rpm during electrospinning. The flow rate was 1 mL h^{-1} through a needle with an inner diameter of 800 µm. The tip-to-collector distance was 14 cm and the electrospinning started by applying a voltage of 20 kV, Fig S1a. After electrospinning, the aluminium collector was pulled off (Fig S1b) and the electrospinning mat can be easily removed for later use.

Stabilization. Also referred to as reticulation or consolidation, the stabilization was performed by putting a piece of the electrospun mat in an air furnace and heating at 120 °C h^{-1} until 290 °C for 2 h stay before 300 °C h^{-1} cooling to room temperature. After this step, the yield is 75-92 wt% depending of the nature of the electrospun mat. This yield can be even low if DMF was not properly removed before the experiment and if the humidity level is high.

Calcination. The sample from the previous step was treated under N_2 in a tubular furnace at 300 °C h^{-1} up to a first dwell (50 °C, 1 h) and slowed down to 120 °C h^{-1} toward the target dwell of 1000 °C for a 2 h stay, followed by 300 °C h^{-1} cooling to room temperature. Initially, a vacuum was achieved (pressure below 0.01 mbar) after the introduction of the sample. The obtained materials are referred to as PAN, PAN-Ni-nitrate, PAN-Ni-acetate, PAN-Ni-sulphate, PAN-Ni-phosphate and PAN-Ni-acetylacetonate for the free-standing electrodes derived from PAN and PAN-Ni with different precursors. After this step, the yield is 40-50 wt% depending of the nature of the pristine electrospun mat that was stabilized in the previous step. The combined yield is then 30-46%.

Physicochemical Characterization. Thermogravimetric analysis (TGA) and differential scanning calorimetry (DSC) were performed with SDT Q600 TA Instruments using aluminium crucibles in the temperature range of room temperature to 800 °C at 5 °C min^{-1} under air flow of 100 mL min^{-1}. Scanning electron microscopy (SEM) observation was performed on a Hitachi S-4800 FEG microscope. Energy dispersive X-ray spectroscopy (EDX) analysis was carried out on a

ZEISS EVOHD 15 microscope. X-ray photoelectron spectroscopy (XPS) characterization was performed on a Thermo Electron ESCALAB 250 spectrometer equipped with a monochromatic radiation source Al Mono ($Al_{k\alpha}$ = 1486.6 eV) operating at 15 kV and 6 mA (survey at a step of 1 eV for transition energy of 150 eV and high-resolution at 0.1 eV for transition energy of 20 eV). The binding energies were corrected on the basis of the energy of C 1s at 284.4 eV by using the AVANTAGE software for peaks fitting. The quantification was carried out from the peak area after correction with a suitable sensitivity factor.

Electrochemical Measurements. The electrochemical measurements were performed using a SP-150 potentiostat (Biologic Science Instruments). The experiments were performed in a conventional three electrode cell. A slide of glassy carbon (GC) with an area of 12.4 cm^2 and a mercury-mercury oxide (MMO) Hg|HgO (KOH 1 M) were used as counter electrode and reference electrode, respectively. Here, the potentials were scaled versus reversible hydrogen electrode (RHE) using the formula $E_{RHE} = E_{MMOE} + x$, with x = 928 mV was obtained from calibrating curve in H_2-saturated 1 M KOH at 25 °C. For the synthesized free-standing electrodes of PAN or PAN-Ni-X (X = nitrate, acetate, sulphate, phosphate, acetylacetonate), the working electrode was made by cutting the parent material into L-shape of 0.5 cm high and 0.5 cm width (geometric area of 0.5 cm^2, not taking into account the 3D structure of the GDE) and enough space on the top for electrical connection with a gold wire. For the commercial catalyst Pt/C (20 wt%, 2 nm, Premetek Co., USA), the catalytic ink was prepared by mixing 130 µL of ultrapure water, 50 µL of ethanol, 20 µL of Nafion (5 wt%) and 5 mg of catalyst powder. The mixture was ultra-sonicated for at least 30 min until obtaining homogenous ink that was drop-casted onto each face of a L-shaped carbon paper (AvCarb MGL190, 190 µm thickness, Fuel Cell Store) electrode of 0.5 cm^2 and the solvent was evaporated under room temperature to reach ca. 0.1 mg per cm^2. The redox probe experiments by $Fe(CN)_6^{3-}/Fe(CN)_6^{4-}$ were conducted with 0.5 M KNO_3 as the electrolyte and 5 mM $K_3[Fe(CN)_6]$ as the substrate. Hydrogen evolution reaction (HER) and oxygen evolution reaction (OER) were performed in 1 M KOH. The used area for the current density was the aforementioned value of 0.5 cm^2. The electrochemically active surface area (ECSA) was determined from the standard method of the electrochemical double-layer capacitance (C_{dl}) of the catalytic surfaces: ECSA = C_{dl}/C_s; C_s = 40 µF cm^{-2} as the average specific capacitance.[1,2]

Table S1. Comparative performance of relevant HER or OER on electrocatalysts synthesized by the electrospinning approach from literature. GCE = Glassy carbon electrode, CPE: carbon paper electrode.

Ref.	Type of materials after electrospinning and thermal treatment	Electrode material testing (free-standing vs ink)		HER or OER Efficiency
		Free-standing?	electrode preparation	
Herein	Ni-containing carbon fibres derived from PAN-Ni NiX_n (ca. 11 wt% Ni), X = counter anion: nitrate, acetate, sulphate, phosphate and acetylacetonate	YES	Working electrode = cutting the parent material into L-shape of 0.5 cm high and 0.5 cm width. Best performance with acetate as the counter anion	HER in 1 M KOH: overpotential of 0.26 V at 10 mA cm^{-2}. OER in 1 M KOH: overpotential of 0.37 V at 10 mA cm^{-2} (1.6 – 1.23 = 0.37 V)
F. Liu, M. Yu, X. Chen, J. Li, H. Liu and F. Cheng, Chin. J. Catal., 2022, 43, 122-129.[3]	High-entropy materials of (MgCoNiCuZn)O	NO	Catalytic ink (catalyst + acetylene black + Nafion + isopropanol) drop-cast onto 1×1 cm^2 CPE to yield 1 mg cm^{-2}	OER in 1 M KOH: overpotential of 360 mV at 10 mA cm^{-2}
J. Li, S. Sun, Y. Yang, Y. Dai, B. Zhang and L. Feng, Chem. Commun., 2022, 58, 9552-9555.[4]	Heterogeneous Ni/Ni2P	NO	Catalytic ink (catalyst + ethanol + Nafion) drop-cast onto 0.07 cm^2 GCE to yield 0.71 mg cm^{-2}	OER in 1 M KOH: overpotential of 0.37 V at 10 mA cm^{-2} (1.6 – 1.23 = 0.37 V)
H. Li, H. Zhu, S. Sun, J. Hao, Z. Zhu, F. Xu, S. Lu, F. Duan and M. Du, Chem. Commun., 2021, 57, 10027-10030.[5]	high-entropy alloy materials of FeCoNiCrMn/CNFs	YES	The FeCoNiCrMn carbon nanofibers were directly cut into a flake of 1×1 cm^2 in area, and were utilized as working electrode	OER in 0.1 M KOH: overpotential of 0.407 V at 50 mA cm^{-2} (1.637 – 1.23 = 0.407 V)
M. Li, H. Wang, W. Zhu, W. Li, C. Wang and X. Lu, Adv. Sci., 2020, 7, Article Number: 1901833.[6]	Ru and Ni nanoparticles embedded within nitrogen-doped carbon nanofibers (RuNi-NCNFs)	NO	Catalytic ink (catalyst + ethanol, + Nafion) drop-casting onto 0.196 cm^2 GCE to yield 0.612 mg cm^{-2}	HER in 1 M KOH: overpotential of 35 mV at 10 mA cm^{-2}. OER in 1 M KOH: overpotential of 0.29 V at 10 mA cm^{-2} (1.23 + 0.29 = 1.52 V vs RHE)
Y. Ao, S. Chen, C. Wang and X. Lu, J. Colloid Int. Sci., 2021, 601, 495-504.[7]	carbon nanofibers embedded with palladium cobalt alloy nanoparticles (PdCo-CNFs)	NO	Catalytic ink (catalyst + ethanol, + water + Nafion) drop-casting onto 0.196 cm^2 GCE to yield 0.2 mg cm^{-2}	HER in 3 M KOH: overpotential of 258 mV at 10 mA cm^{-2}
Y. Zhang, D. Kong, L. Bo, W. Shi, X. Guan, Y. Wang, Z. Lei and J. Tong, ACS Appl. Energy Mater., 2021, 4, 13051-13060.[8]	N, P-doped MoC, Mo2C, and porous carbon fibers	NO	Catalytic ink (catalyst + ethanol + Nafion) drop-casting onto 0.07 cm^2 GCE to yield 0.69 mg cm^{-2}	HER in 0.5 M H_2SO_4: overpotential of 125 mV at 10 mA cm^{-2}
Y.-X. Xiao, J. Ying, J.-B. Chen, Y. Dong, X. Yang, G. Tian, J. Wu, C. Janiak,	Pt-NPs in N-doped porous carbon fibers (Pt@NDPCF)	NO	Catalytic ink (catalyst + isopropanol + Nafion + water) drop-cast onto GCE	HER in 0.1 M $HClO_4$: overpotential of 35 mV at 10 mA cm^{-2}

K. I. Ozoemena and X.-Y. Yang, Chem. Mater., 2022, 34, 3705-3714.[9]				
F. Qiang, J. Feng, H. Wang, J. Yu, J. Shi, M. Huang, Z. Shi, S. Liu, P. Li and L. Dong, ACS Catal., 2022, 12, 4002-4015.[10]	N-doped porous carbon nanofibers (NPCNFs-O)	NO	Catalytic ink (catalyst + ethanol + Nafion + water) drop-cast onto GCE to yield 0.9 mg cm^{-2}	OER in 1 M KOH: overpotential of 326 mV at 10 mA cm^{-2}
A. Wang, Y. Hu, H. Wang, Y. Cheng, T. Thomas, R. Ma and J. Wang, Mater. Today Phys., 2021, 17, 100353.[11]	Spinel NiCo2O4 Embedded in N-doped Carbon Nanofibers (carbon content is ∼63 wt%)	NO	Catalytic ink (catalyst + ethanol + Nafion + water) drop-cast onto GCE to yield 0.5 mg cm^{-2}	OER in 0.1 M KOH: overpotential of 370 mV at 10 mA cm^{-2} (1.6 – 1.23 = 0.37 V)
L. Fan, Q. Li, D. Wang, T. Meng, M. Yan, Z. Xing, E. Wang and X. Yang, Chem. Commun., 2020, 56, 739-742.[12]	Electrospun Ru–RuO2/MoO3 carbon nanorods	NO	Catalytic ink (catalyst + DMF + Nafion) drop-cast onto CPE (0.5 ×0.6 cm^2) to yield 0.261 mg cm^{-2}	HER in 1 M KOH: overpotential of 10 mV at 10 mA cm^{-2}
D. Xie, G. Yang, D. Yu, Y. Hao, S. Han, Y. Cheng, F. Hu, L. Li, H. Wei and C. Ji, ACS Sustainable Chem. Eng., 2020, 8, 14179-14189. [13]	MoS2 nanosheets functionalized multichannel hollow carbon nanofibers containing Mo2N (Mo2N−MoS2 MCNFs)	NO	Catalytic ink (catalyst + Super P + PVDF + NMP) drop-casting onto 1 × 2 cm^2 Ni foam to yield 1 mg cm^{-2}	HER in 1 M KOH: overpotential of 131 mV at 10 mA cm^{-2}. OER in 1 M KOH: overpotential of 270 mV at 10 mA cm^{-2}
Y. Zhao, J. Zhang, K. Li, Z. Ao, C. Wang, H. Liu, K. Sun and G. Wang, J. Mater. Chem. A, 2016, 4, 12818-12824.[14]	cobalt nanoparticle embedded porous nitrogen doped carbon nanofibers (Co-PNCNFs)	NO	Catalytic ink (catalyst + Nafion + isopropanol + water) drop-casting onto 0.07 cm^2 GCE to yield 0.56 mg cm^{-2}	HER in 1 M KOH: overpotential of 249 mV at 10 mA cm^{-2}. OER in 1 M KOH: overpotential of 285 mV at 10 mA cm^{-2}
S. Surendran, S. Shanmugapriya, A. Sivanantham, S. Shanmugam and R. Kalai Selvan, Adv. Energy Mater., 2018, 8, 1800555.[15]	Electrospun Carbon Nanofibers Encapsulated with NiCoP	NO	Catalytic ink (catalyst + carbon black + polyvinylidene + N-methyl 2-pyrrolidine) drop-casting onto carbon cloth substrate	HER in 1 M KOH: overpotential of 130 mV at 10 mA cm^{-2}. OER in 1 M KOH: overpotential of 268 mV at 10 mA cm^{-2}
X. Wang, Y. Li, T. Jin, J. Meng, L. Jiao, M. Zhu and J. Chen, Nano Lett., 2017, 17, 7989-7994.[16]	Thin-Walled CuCo2O4@C Nanotubes (carbon content: 19.64 wt %)	NO	Catalytic ink (catalyst + ethanol + isopropanol + Nafion) drop-casting onto 0.12 cm^2 GCE to yield 0.28 mg cm^{-2}	OER in 1 M KOH: overpotential of 327 mV at 10 mA cm^{-2}

Table S2. EDX analysis of the different materials derived from different precursors of Ni(+II): Electrospun PAN follows by thermal treatment: stabilization at 290 °C (under air) calcination at 1000 °C (under N_2).

Note: "± 0.1" means that the SD was below that, for example, "0.2 ± 0.1" is in fact "0.21 ± 0.06".

Entry		PAN-Ni-nitrate	PAN-Ni-acetate	PAN-Ni-sulphate	PAN-Ni-phosphate	PAN-Ni-acetylacetonate	Control (PAN)
Weight	C(wt%)	89.6 ± 0.2	85.4 ± 0.3	80.0 ± 0.1	71.7 ± 0.2	79.0 ± 0.1	97.3 ± 0.8
	N(wt%)	0.2 ± 0.1	2.8 ± 0.4	5.8 ± 0.2	6.8 ± 0.3	6.3 ± 0.3	1.7 ± 0.3
	O(wt%)	1.4 ± 0.1	2.0 ± 0.1	4.4 ± 0.1	4.2 ± 0.1	3.4 ± 0.1	1.0 ± 0.1
	S(wt%)			0.8 ± 0.1			
	P(wt%)				4.4 ± 0.1		
	Ni(wt%)	8.7 ± 0.1	9.5 ± 0.1	8.9 ± 0.2	11.8 ± 0.1	11.0 ± 0.3	
Atomic	C(at%)	96.8 ± 0.2	93.4 ± 0.2	88.5 ± 0.3	84.0 ± 0.3	88.3 ± 0.2	97.3 ± 0.8
	N(at%)	0.2 ± 0.1	2.6 ± 0.2	5.5 ± 0.3	6.8 ± 0.3	6.2 ± 0.3	1.7 ± 0.3
	O(at%)	1.2 ± 0.1	1.7 ± 0.3	3.6 ± 0.1	3.7 ± 0.1	2.9 ± 0.3	1.0 ± 0.1
	S(at%)			0.4 ± 0.1			
	P(at%)				1.9 ± 0.1		
	Ni(at%)	1.9 ± 0.1	2.1 ± 0.1	2.0 ± 0.1	2.8 ± 0.1	2.5 ± 0.1	
Atomic ratio	C/N	509 ± 20	36 ± 5	16 ± 7	12 ± 3	14 ± 1	58 ± 4
	Ni/P				1.8		

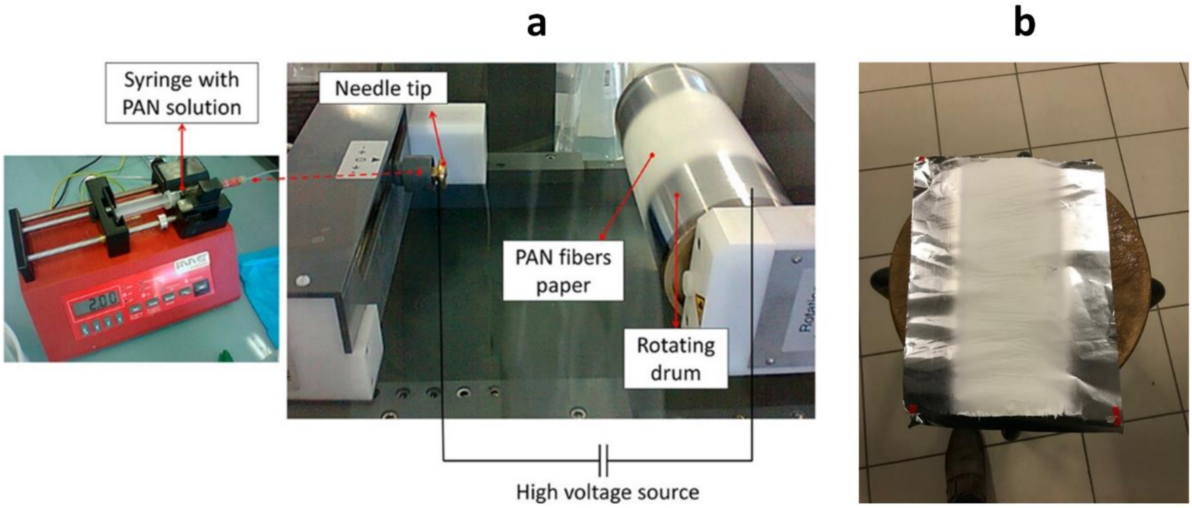

Fig. S1. Home-made electrospinning setup for the fabrication of electrospun fibers fabrication. (a) Photographs of the apparatus (courtesy of Adriana Both Engel, Copyright 2015)[17] and (b) photograph of as-fabricated electrospun mat.

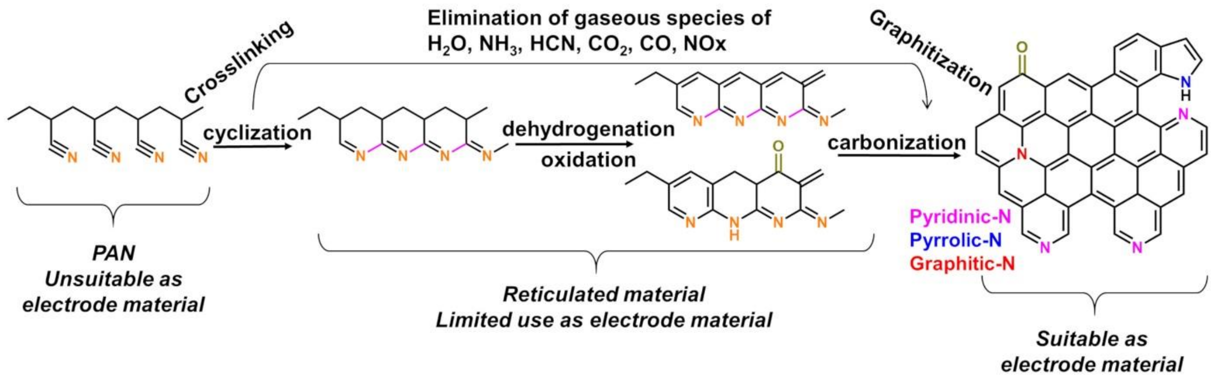

Fig. S2. Sketch of the thermal treatment starting from polyacrylonitrile-based material to the fabrication of an electrode material.[18]

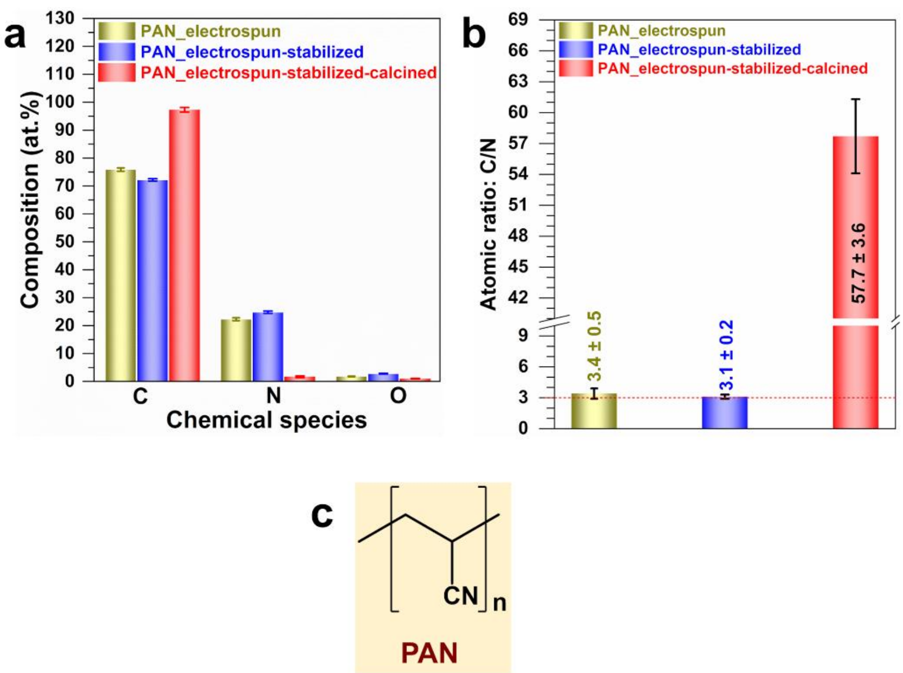

Fig. S3. EDX analysis of PAN at different stages: electrospinning, stabilization and calcination (a) Atomic composition as-determined from EDX. (b) atomic ratio of C/N as-determined from EDX. (c) Formula of PAN.

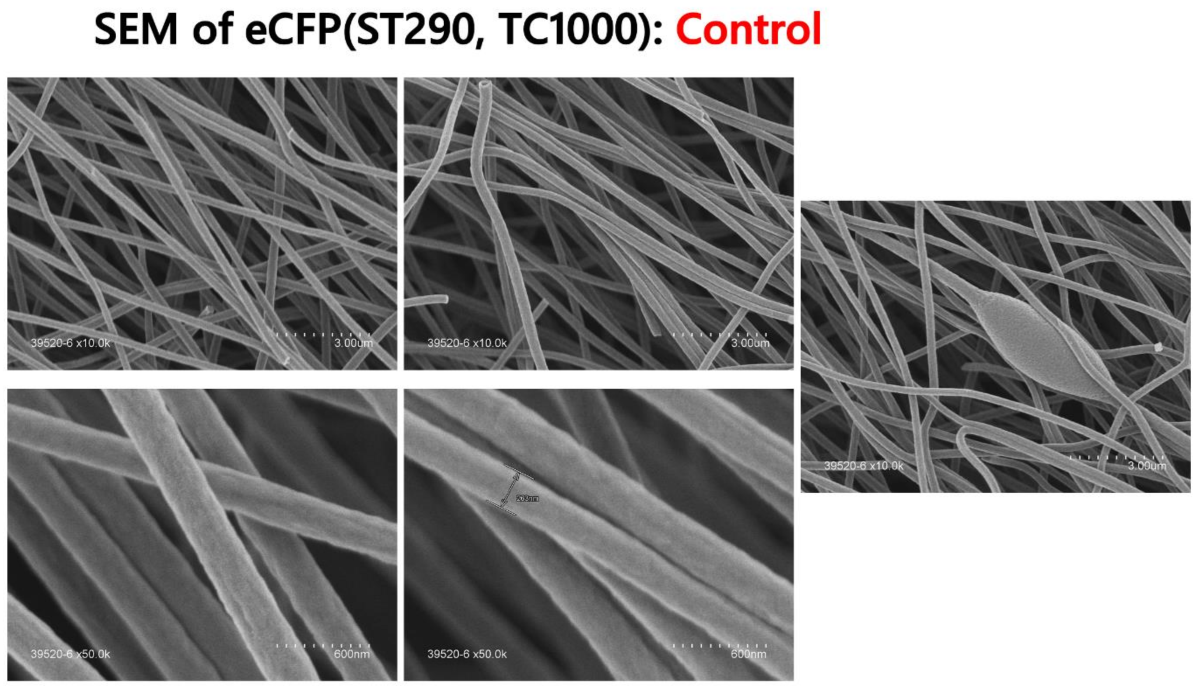

Fig. S4. SEM images at different magnifications for the material derived from electrospun PAN after thermal treatment: TS290 for stabilization at 290 °C (under air) and TC1000 for calcination at 1000 °C (under N_2).

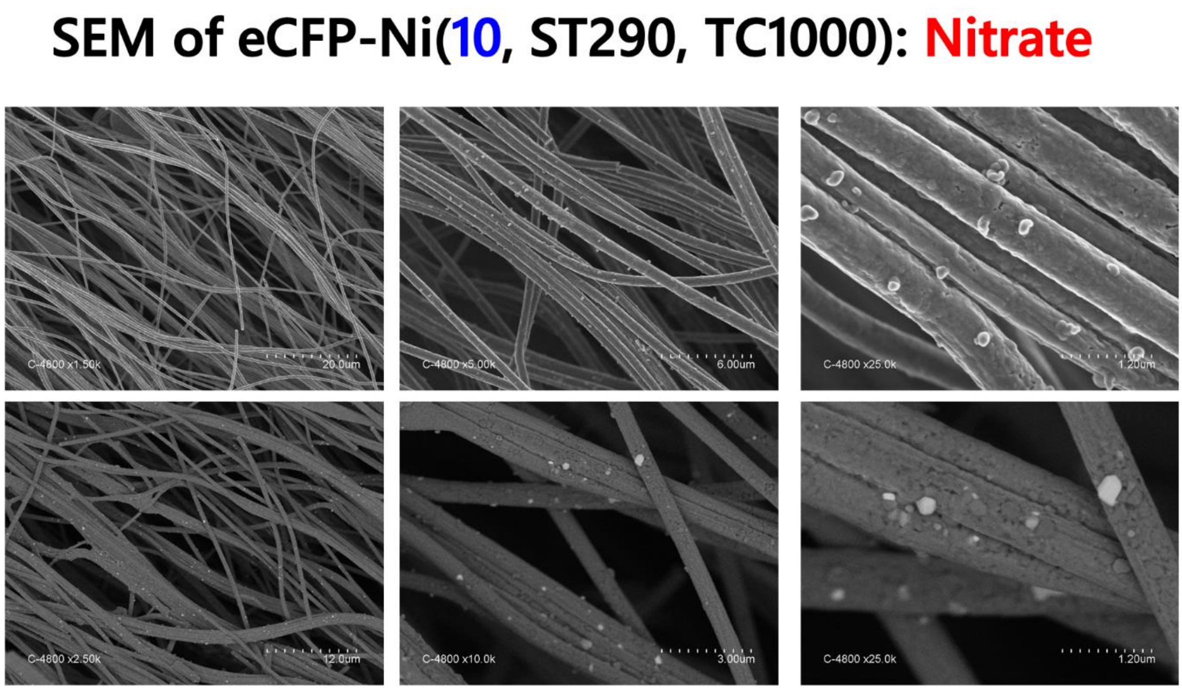

Fig. S5. SEM images at different magnifications for the material derived from electrospun PAN-Ni-nitrate after thermal treatment: TS290 for stabilization at 290 °C (under air) and TC1000 for calcination at 1000 °C (under N_2).

SEM of eCFP-Ni(10, ST290, TC1000): Acetate

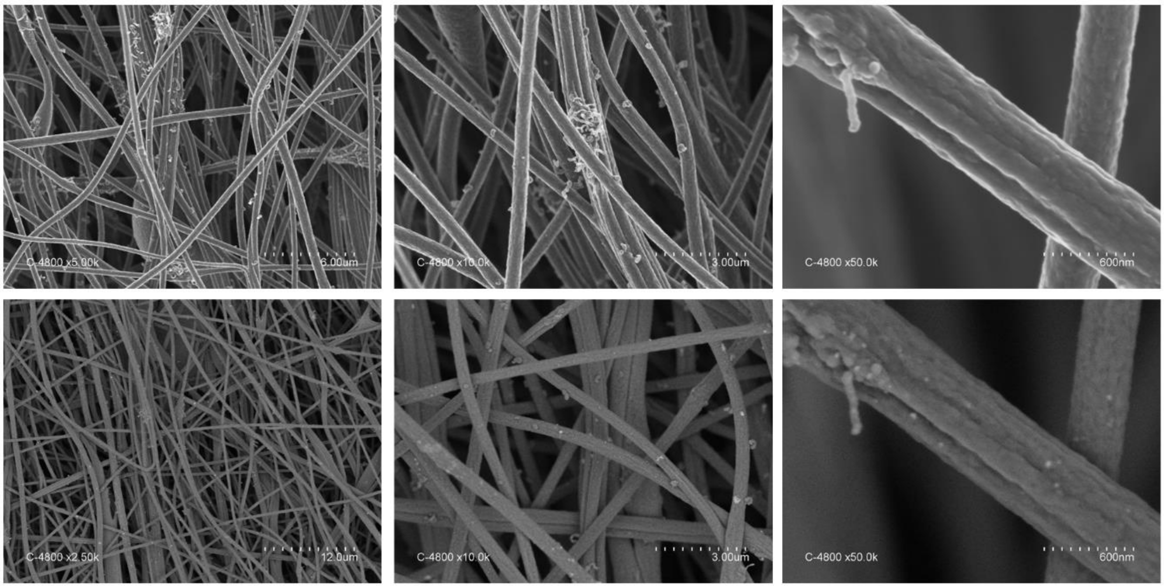

Fig. S6. SEM images at different magnifications for the material derived from electrospun PAN-Ni-acetate after thermal treatment: TS290 for stabilization at 290 °C (under air) and TC1000 for calcination at 1000 °C (under N_2).

SEM of eCFP-Ni(10, ST290, TC1000): Sulphate

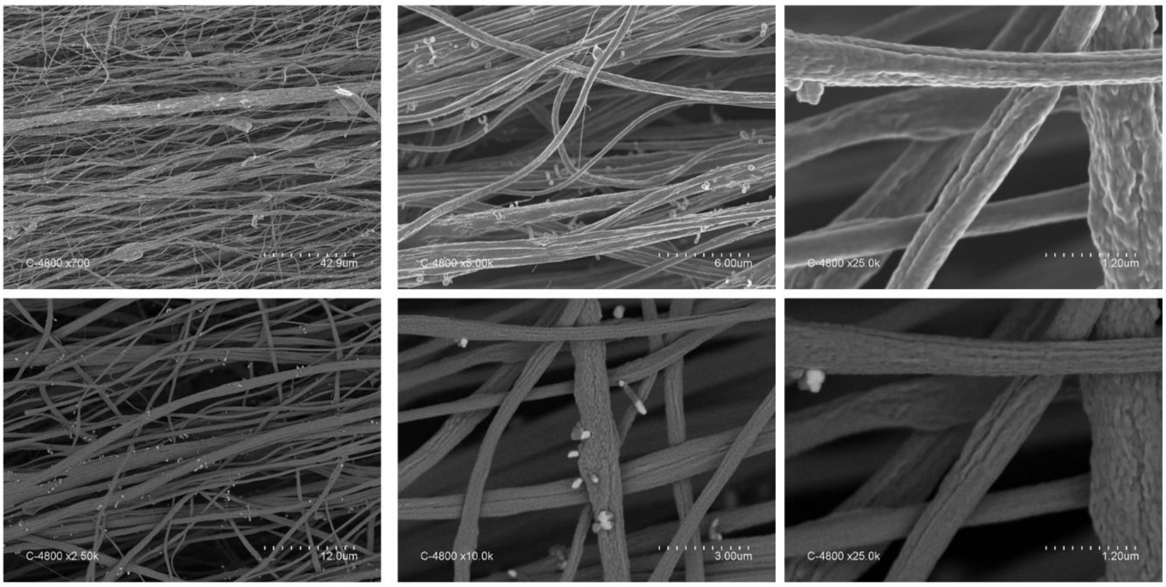

Fig. S7. SEM images at different magnifications for the material derived from electrospun PAN-Ni-sulphate after thermal treatment: TS290 for stabilization at 290 °C (under air) and TC1000 for calcination at 1000 °C (under N_2).

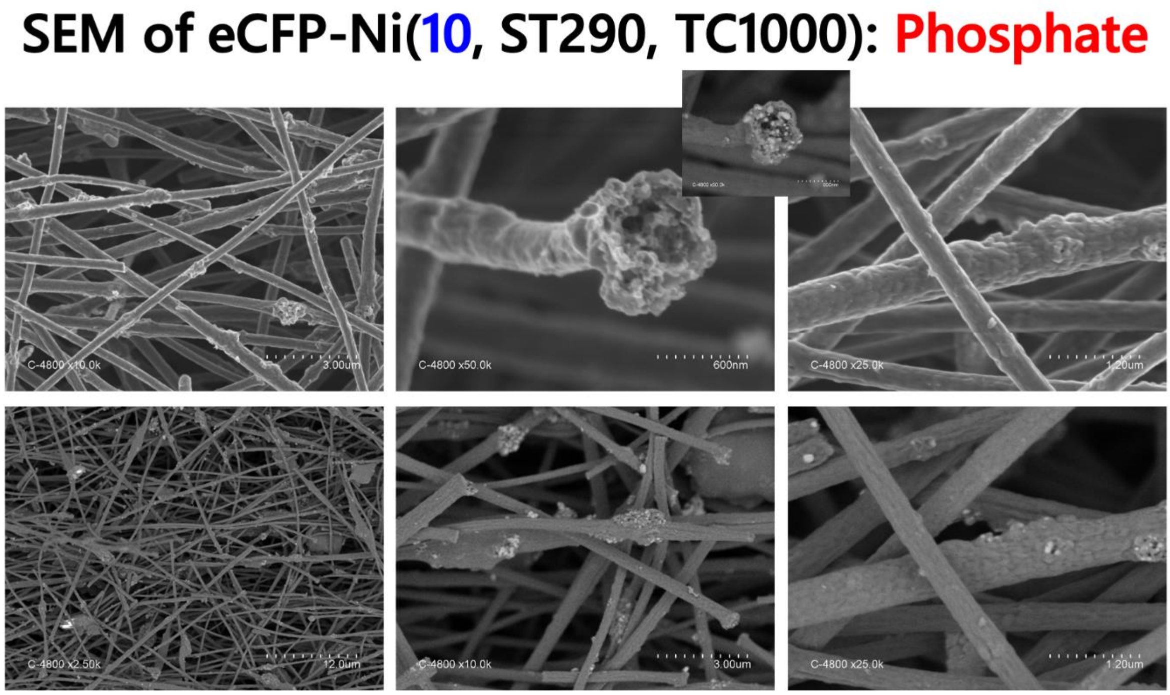

Fig. S8. SEM images at different magnifications for the material derived from electrospun PAN-Ni-phosphate after thermal treatment: TS290 for stabilization at 290 °C (under air) and TC1000 for calcination at 1000 °C (under N_2).

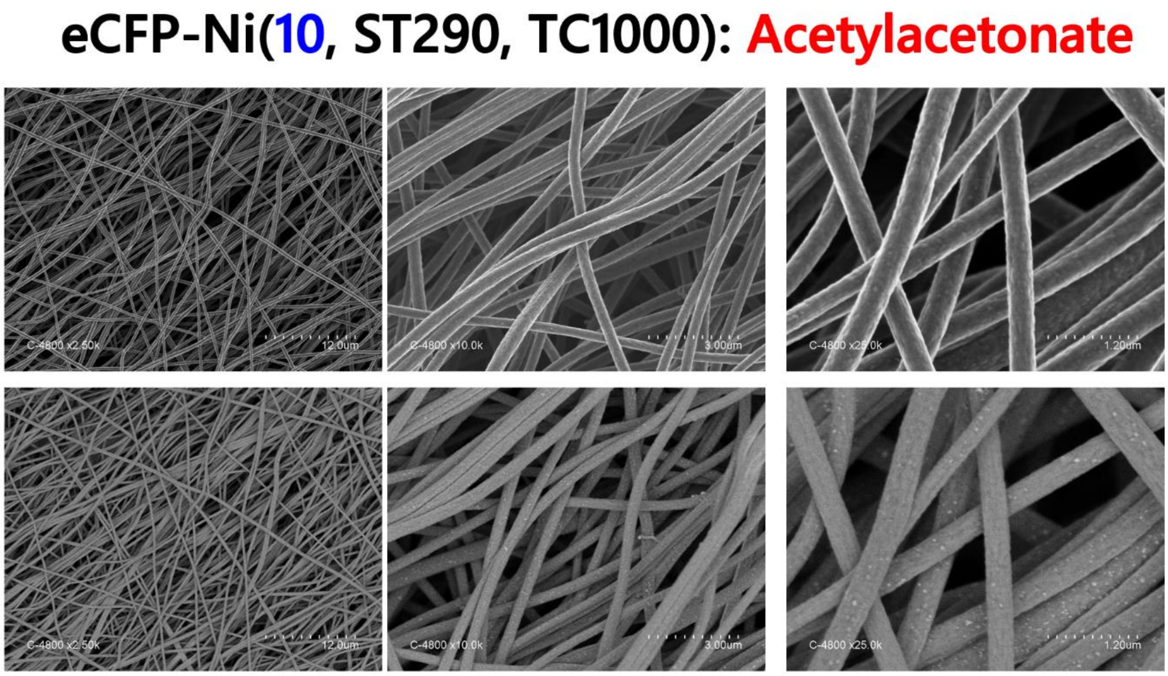

Fig. S9. SEM images at different magnifications for the material derived from electrospun PAN-Ni-acetylacetonate after thermal treatment: TS290 for stabilization at 290 °C (under air) and TC1000 for calcination at 1000 °C (under N_2).

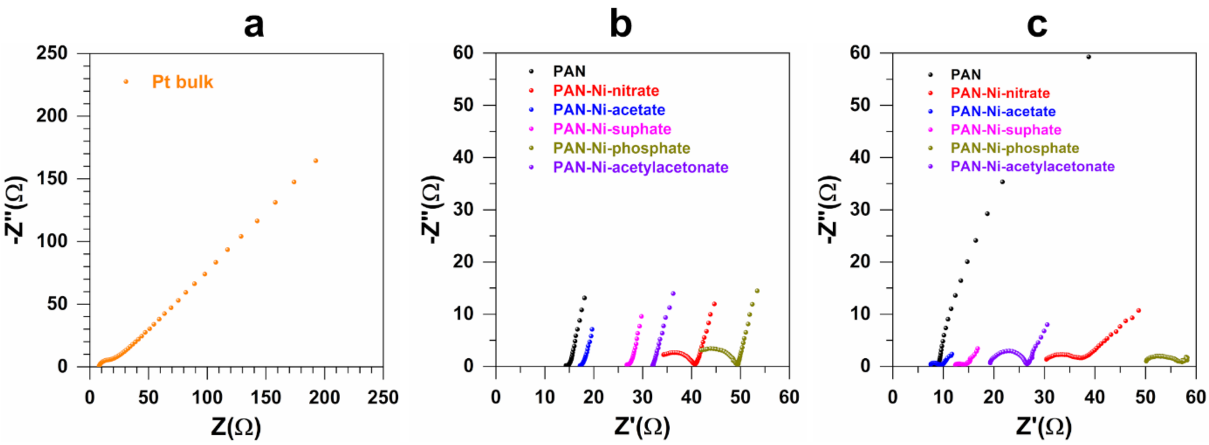

Fig. S10. Complex-plane Nyquist impedance from EIS results in 0.5 M KNO_3 + 5 mM $K_3[Fe(CN)_6]$ and 1 M KOH at and 25 °C.

(a) Qualification with Pt bulk (ca. 0.5 cm^2) in 0.5 M KNO_3 + 5 mM $K_3[Fe(CN)_6]$ at open circuit potential (OCP) of 0.2 V vs SCE to double-check the behavior. **(b, c)** 0.5 cm^2 electrodes derived from PAN, PAN-Ni-nitrate, PAN-Ni-acetate, PAN-Ni-sulphate, PAN-Ni-phosphate, and PAN-Ni-acetylacetonate: **(b)** at OCP of 0.2 V vs SCE in 0.5 M KNO_3 + 5 mM $K_3[Fe(CN)_6$ and 25 °C and **(c)** at -0.3 V vs RHE in 1 M KOH and 25 °C. The uncompensated ohmic resistance (R_{Ω}) that includes contribution from the connections, electrolyte, and working electrode material is the intersection between the Nyquist curve and x axis at low impedance.

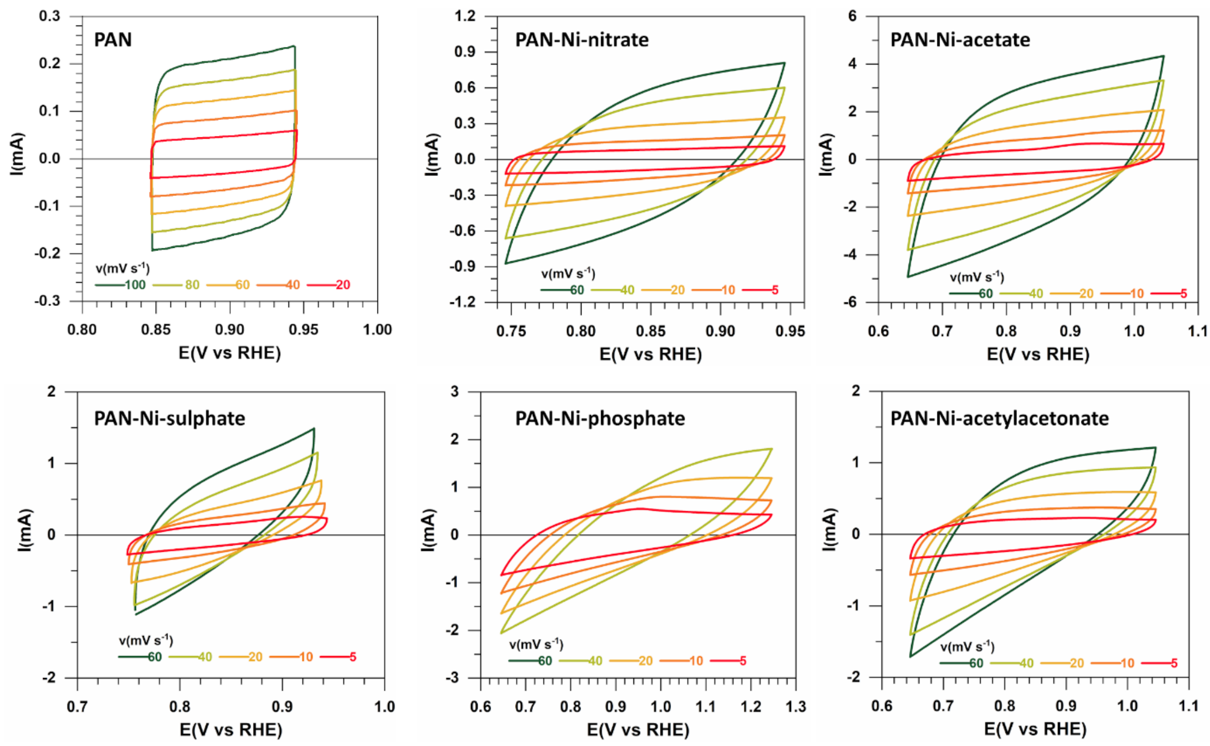

Fig. S11. Double-layer capacitance measurements for determining electrochemically active surface area (ECSA): iR-drop uncorrected CV (1 M KOH, 25 °C) for determining ECSA.

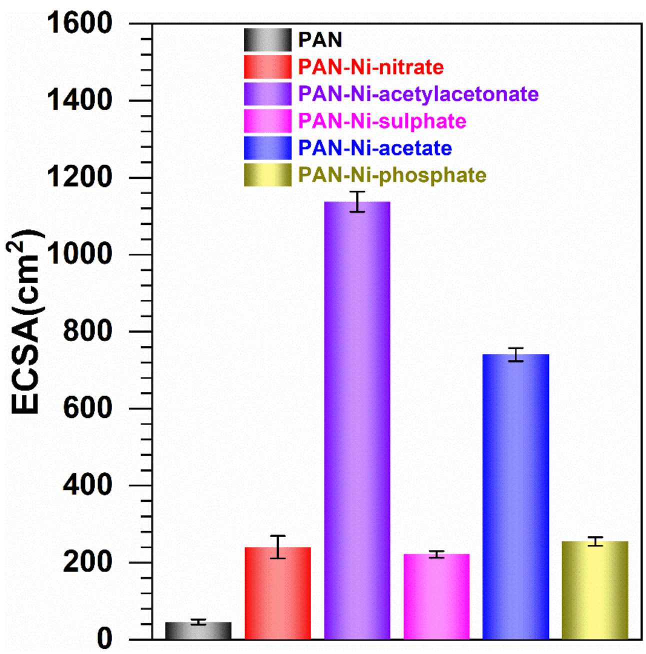

Fig. S12. Determined electrochemically active surface area (ECSA) from the double-layer capacitance measurements in N_2-saturated 1 M KOH at 25 °C. 0.5 cm^2 electrodes derived from PAN, PAN-Ni-nitrate, PAN-Ni-acetate, PAN-Ni-sulphate, PAN-Ni-phosphate, and PAN-Ni-acetylacetonate.

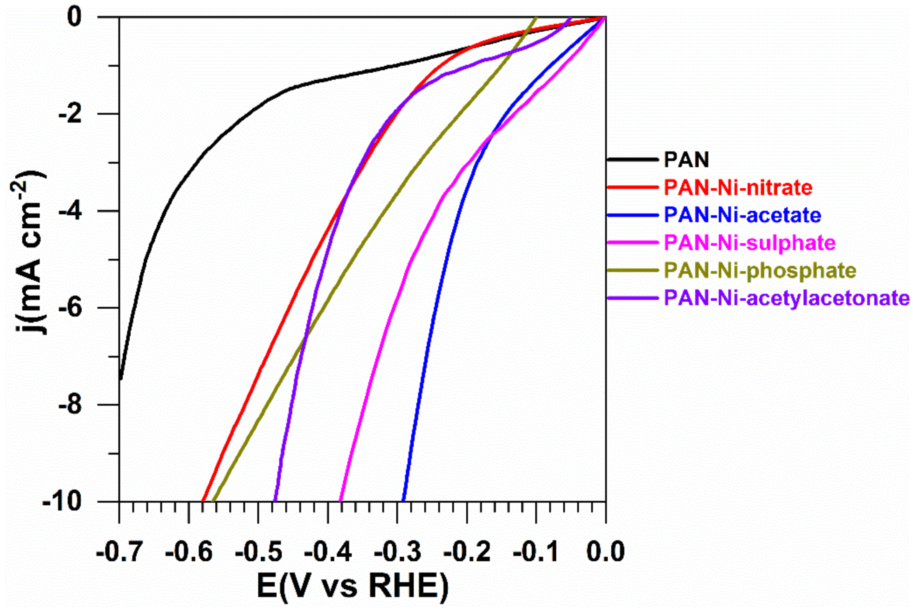

Fig. S13. iR-drop uncorrected LSV of HER (N_2-saturated 1 M KOH, 25 °C, 5 mV s^{-1}).

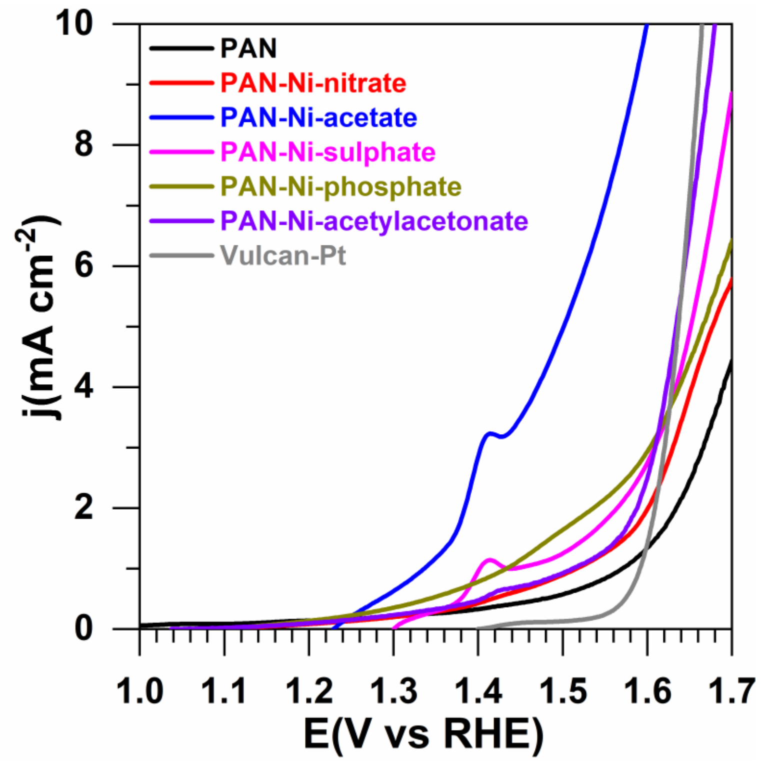

Fig. S14. iR-drop corrected LSV of OER (N_2-saturated 1 M KOH, 25 °C, 5 mV s^{-1}).

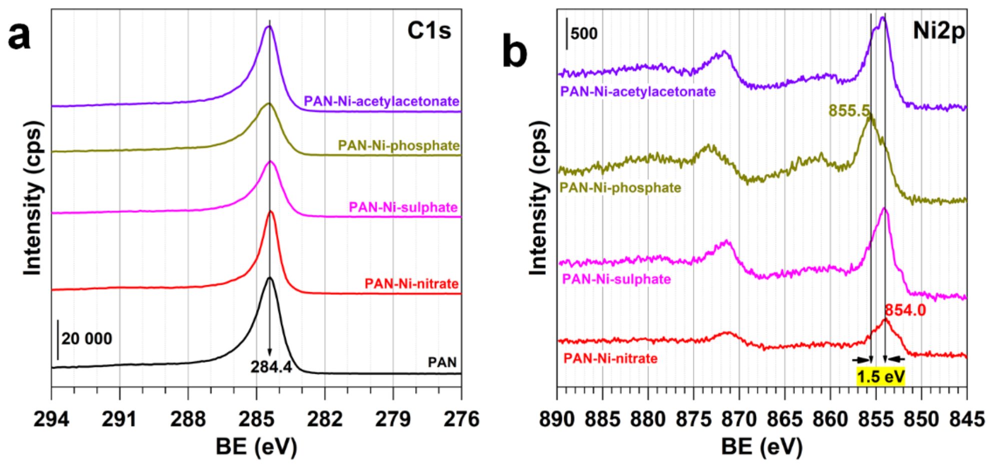

Fig. S15. High-resolution XPS spectra of C 1s and Ni 2p.

(a) C 1s. **(b)** Ni 2p.

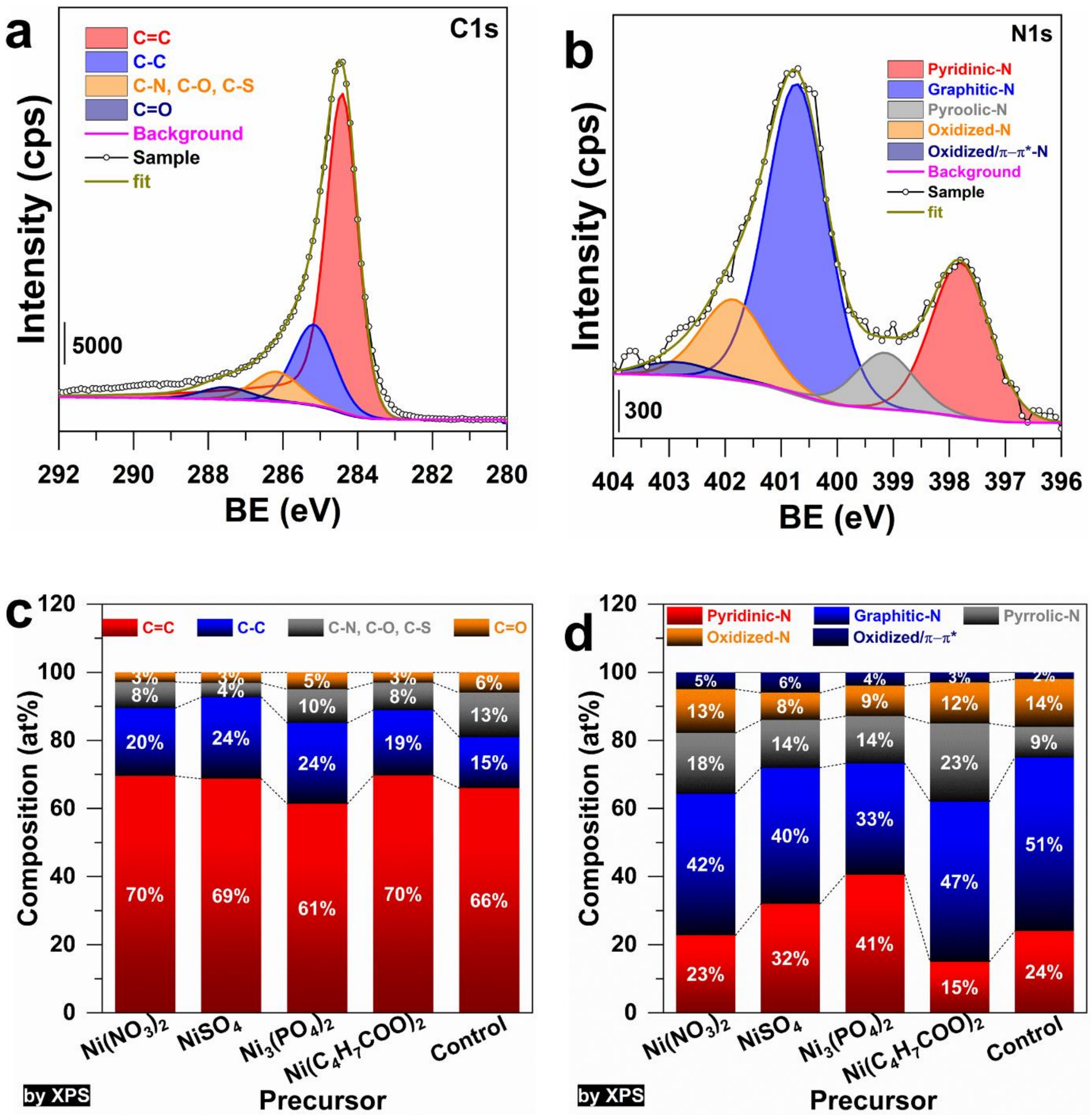

Fig. S16. XPS analysis of C and N.

(a, b) Typical high-resolution spectra of: **(a)** C 1s and **(b)** N 1s. **(c, d)** Overall surface atomic composition of: **(c)** N-based species and **(d)** C-based species

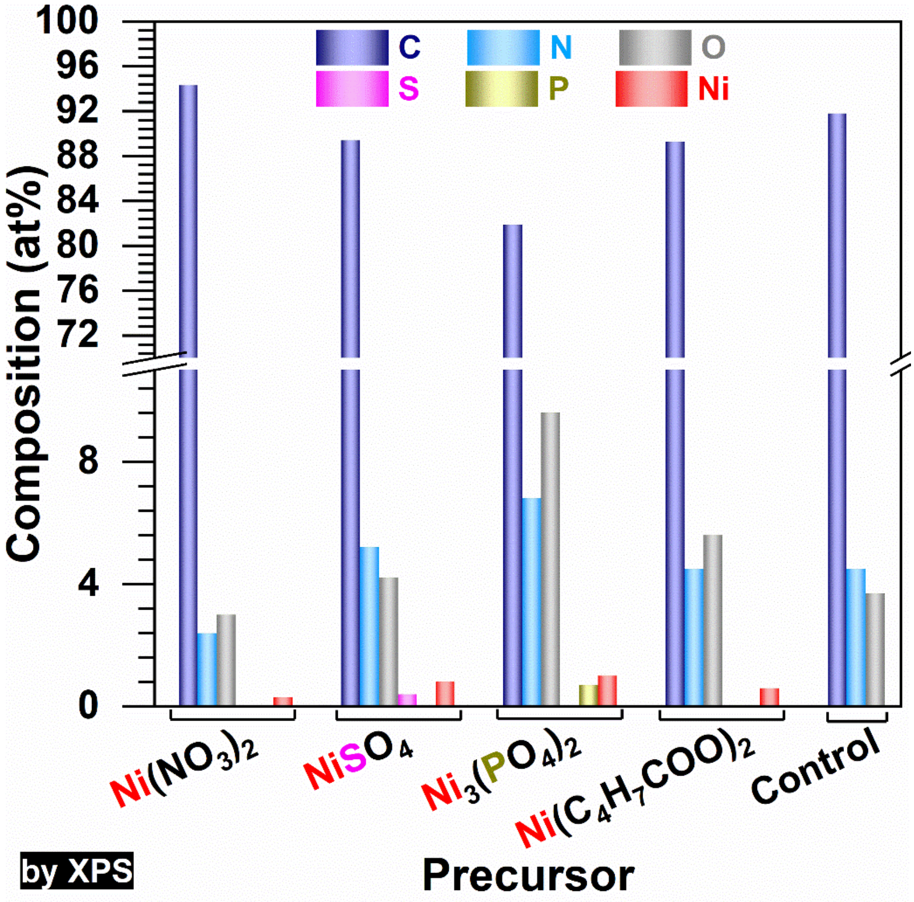

Fig. S17. Overall atomic composition by XPS.

Supplementary References.

1. C. C. L. McCrory, S. Jung, J. C. Peters and T. F. Jaramillo, *J. Am. Chem. Soc.*, 2013, **135**, 16977-16987.
2. S. Trasatti and O. A. Petrii, *J. Electroanal. Chem.*, 1992, **327**, 353-376.
3. F. Liu, M. Yu, X. Chen, J. Li, H. Liu and F. Cheng, *Chin. J. Catal.*, 2022, **43**, 122-129.
4. J. Li, S. Sun, Y. Yang, Y. Dai, B. Zhang and L. Feng, *Chem. Commun.*, 2022, **58**, 9552-9555.
5. H. Li, H. Zhu, S. Sun, J. Hao, Z. Zhu, F. Xu, S. Lu, F. Duan and M. Du, *Chem. Commun.*, 2021, **57**, 10027-10030.
6. M. Li, H. Wang, W. Zhu, W. Li, C. Wang and X. Lu, *Adv. Sci.*, 2020, **7**, Article Number: 1901833.
7. Y. Ao, S. Chen, C. Wang and X. Lu, *J. Colloid Int. Sci.*, 2021, **601**, 495-504.
8. Y. Zhang, D. Kong, L. Bo, W. Shi, X. Guan, Y. Wang, Z. Lei and J. Tong, *ACS Appl. Energy Mater.*, 2021, **4**, 13051-13060.
9. Y.-X. Xiao, J. Ying, J.-B. Chen, Y. Dong, X. Yang, G. Tian, J. Wu, C. Janiak, K. I. Ozoemena and X.-Y. Yang, *Chem. Mater.*, 2022, **34**, 3705-3714.
10. F. Qiang, J. Feng, H. Wang, J. Yu, J. Shi, M. Huang, Z. Shi, S. Liu, P. Li and L. Dong, *ACS Catal.*, 2022, **12**, 4002-4015.
11. A. Wang, Y. Hu, H. Wang, Y. Cheng, T. Thomas, R. Ma and J. Wang, *Mater. Today Phys.*, 2021, **17**, 100353.
12. L. Fan, Q. Li, D. Wang, T. Meng, M. Yan, Z. Xing, E. Wang and X. Yang, *Chem. Commun.*, 2020, **56**, 739-742.
13. D. Xie, G. Yang, D. Yu, Y. Hao, S. Han, Y. Cheng, F. Hu, L. Li, H. Wei and C. Ji, *ACS Sustainable Chem. Eng.*, 2020, **8**, 14179-14189.
14. Y. Zhao, J. Zhang, K. Li, Z. Ao, C. Wang, H. Liu, K. Sun and G. Wang, *J. Mater. Chem. A*, 2016, **4**, 12818-12824.
15. S. Surendran, S. Shanmugapriya, A. Sivanantham, S. Shanmugam and R. Kalai Selvan, *Adv. Energy Mater.*, 2018, **8**, 1800555.
16. X. Wang, Y. Li, T. Jin, J. Meng, L. Jiao, M. Zhu and J. Chen, *Nano Lett.*, 2017, **17**, 7989-7994.
17. A. Both Engel, Y. Holade, S. Tingry, A. Cherifi, D. Cornu, K. Servat, T. W. Napporn and K. B. Kokoh, *J. Phys. Chem. C*, 2015, **119**, 16724-16733.
18. M. Coronas, Y. Holade and D. Cornu, *Materials*, 2022, **15**, article number: 4336.